JOURNAL OF PHOTOPOLYMER SCIENCE AND TECHNOLOGY

http://www.ao.u-tokai.ac.jp/photopolymer/p.htm

Journal of Photopolymer Science and Technology publishes papers on the scientific progress and the technical development of photopolymers.

Editorial Board

International Advisory Board

The Editorial Office

c/o Prof. Kenichiro NAKAMURA
Department of Electro Photo Optics, Tokai University
Kitakaname, Hiratsukashi, Kanagawa 259-1292, Japan.
TEL +81-463-50-2156
FAX +81-463-59-2594
e-mail nakamura@keyaki.cc.u-tokai.ac.jp

Information for Contributors

Submit manuscripts (1 original and 2 copies + ELECTRONIC FILE) with the Contribution Form to The Editorial Office, Journal of Photopolymer Science and Technology, c/o Prof. Kenichiro NAKAMURA, Department of Electro Photo Optics, Tokai University, Kitakaname, Hiratsukashi, Kanagawa 259-1292, Japan. Submission is a representation that the manuscript has not been published previously nor currently submitted for publication elsewhere. The manuscript should be accompanied by a statement transferring copyright from the authors (or their employers-whoever holds the copyright) to The Technical Association of Photopolymers, Japan. A suitable form for copyright transfer is occasionally printed in the back of this journal and is available from the Editorial Office. This written transfer of copyright, which previously was assumed to be implicit in the act of submitting a manuscript, is necessary under the Japan copyright law. Further information may be obtained from the Editorial Office. Contribution Forms are available from the Editorial Office.

Proofs and all correspondence concerning papers in the process of publication should be addressed to the Editorial office.

Manuscript Preparation All the papers submitted are reproduced photographically as they were. For this reason, the manuscripts should be prepared according to the Manual for Manuscript Writings which is occasionally printed in the back of this journal and is available from the Editorial Office.

Subscription Price

(Airmail Postage included)	Japan	Foreign
	¥12,000	US$100.00

Backnumber prices Single Volumes:¥12,000(US$100) (Airmail Postage included)

Subscriptions, renewals, address changes, and backnumber orders should be addressed to the Editorial Office. For address changes please send both old and new addresses and, if possible, include a mailing label from the wrapper of recent issue. Requests from subscribers for missing journal issues will be honored without charge only if received within six months of the issue's actual date of publication; otherwise, the issue may be purchased at the single-copy price.

Publication Charge (Reprint Order) To support a part of the cost of publication of journal pages, the author's institution is requested to pay a page charge of ¥3,000(US$25) per page (with a one-page minimum) and an article charge of ¥10,000(US$100) per article. The page charge (if honored) entitles the author to 100 free reprints. For Errata the minimum page charge is ¥1,200(US$10), with no article charge and no free reprints.

The cover designed by M.Tsuda and M.Morishita

JOURNAL OF PHOTOPOLYMER SCIENCE AND TECHNOLOGY

Volume 17 Number 4

2004

Published by

THE TECHNICAL ASSOCIATION OF PHOTOPOLYMERS

JAPAN

Review

Journal of Photopolymer Science and Technology
Volume17, Number4(2004)587-602©2004TAPJ

193 nm Immersion Lithography – Taking the Plunge

Ralph R. Dammel, Frank M. Houlihan, Raj Sakamuri, David Rentkiewicz, and Andrew Romano,

AZ Electronic Materials, Clariant Corporation, 70 Meister Avenue, Somerville, NJ 08876, USA

This paper reviews the current status and future outlook of materials for 193 nm immersion lithography, with special focus on top barrier layers, photoresists, bottom antireflective coatings for numerical apertures exceeding unity, and future challenges for imaging materials along the Roadmap.

Keywords: immersion lithography, 193 nm lithography, antireflecting coating, flavored water

1. Introduction

In the last eighteen months, 193 nm immersion lithography has changed from an outside possibility to the declared front runner for the successor technology to 193 nm dry lithography. It has become the front-up technology for the 45 nm node on the International Technology Roadmap for Semiconductors (ITRS), displacing 157 nm technology to a back-up position in the process.

This paper focuses on the materials issues associated with the introduction of 193 nm immersion technology, most specifically the issues raised by immersion lithography for photoresists as well as anti-reflective and barrier coatings. These issues are on the one side related to the exposure of the imaging stack to aqueous immersion media (either water or higher refractive index versions of "flavored" water), on the other side to the effects of the super-high numerical apertures and the correspondingly highly oblique angles of incidence that will result from the exposure of small features.

Issues arising from the exposure of the imaging stack to an aqueous immersion medium can be generally classified in the areas of penetration of the immersion medium into the imaging stack, and leaching or dissolution of imaging stack components into the immersion medium. In the most general case, the imaging stack is composed of an anti-reflective bottom coating or underlayer, a photoresist, and a top barrier layer or top antireflective coating.

- Recent developments in top barrier layers have resulted in more user friendly materials that are developer soluble and add only minimal process complexity, while being almost 100% effective in eliminating leaching effects.
- Photoresist materials based on the dominant platform for dry lithography, (meth)acrylate systems, have been shown to work unexpectedly well even without the use of a top barrier layer, although in that case their performance still lags behind that of dry lithography. However, it can already be anticipated that optimization of the methacrylate polymer platform will lead to its successful extension to 193 nm immersion lithography. Optimization is also required for bases, photoacid generators, and additives to achieve the best performance.
- In the area of bottom coats, the main issue is the changes brought by a greatly expanded range of angles of incidence, from near vertical for large features to, say, 45% near the resolution limit of a 1.2 NA scanner. Optimum BARC thickness changes as the inverse of the cosine of the angle of refraction into the BARC, so that a homogeneous single layer BARC will not be able to adequately suppress reflectivity effects for all angles. More complex solutions are required, such as multilayer or graded BARCS.

Lastly, the development of materials for immersion lithography will have to deal with the issues caused by ever rising requirements along the roadmap, e.g., specifications for line edge roughness (LER), PEB sensitivity, defectivity, etc. It is currently still unclear whether and if yes, to what extent immersion technology will exacerbate these phenomena. One area where immersion lithography is already known to have an issue is the collapse of fine line structures, which is more severe in 193 nm resists than in 157 nm lithography, presumably due to a difference in the hydrophobicity of developed

Received May 19, 2004

resist structures and hence in their contact angle. The collapse phenomenon may very well enforce the use of aspect ratios well below 3, with the obvious repercussions for dry etch processes. There is also growing evidence that these thin films will become subject to confinement effects[1] in which properties of the resist such as diffusivity or glass transition temperature increasingly deviate from their bulk values as resist film thickness falls below a critical value. Resist design will have to be aware of these effects and take them into account.

2. Penetration of Water into Photoresists

Penetration of water into the photoresist is of interest because water can change both the optical and chemical properties of the photoresist. Studies of water uptake have so far been carried out only for resist layers unprotected by a top barrier coating, with the general assumption that such a coating will be designed to prevent diffusion of water into the photoresist, at least for the lengths of time currently under consideration for the immersion step.

A general study of the water uptake of photoresist polymers coated onto wafers has been carried out using a combination of quartz crystal microbalance and interferometric methods.[2] All polymers studied (Fig. 1) were found to take up varying amounts of water, with water uptake saturation values mostly in the range of 0.4%. One exception is poly(hydroxystyrene), which takes up almost ten times as much water, in very rough agreement with a study investigating water uptake from the gas phase that found a saturation value of 9.6%.[3] The water uptake of a commercial 248 nm resist (UV II, based on a hydroxystyrene/t-butyl acrylate copolymer) is, however, found to be comparable to that of the lower tier polymers.

The mathematical description of Fickian diffusion into a polymer layer is given by Crank[4] for the case of a free-standing polymer sheet. It can be shown that due to the re-normalization to mass uptake at infinite time and to the symmetry properties at the center of the free-standing sheet, the solutions are also valid for a thin film coated on a wafer.

Crank's solution of the diffusion equations for a film of thickness L (or a free-standing film of thickness 2 L) with diffusion constant D gives a normalized mass uptake of

$$\frac{M(t)}{M_\infty} = 1 - \frac{8}{\pi}\sum_{m=0}^{\infty}\frac{1}{(2m+1)^2}\exp\left[-D\cdot(2m+1)^2\pi^2\frac{t}{L^2}\right] \quad (1)$$

with the resulting concentration in the polymer film given by

$$\frac{C}{C_0} = 1 - \frac{4}{\pi}\sum_{m=0}^{\infty}\frac{(-1)^n}{2n+1}\exp\left[-D\cdot(2n+1)^2\frac{\pi^2}{4}\frac{t}{L^2}\right]\cdot \cos\left[\frac{(2n+1)\pi x}{2L}\right] \quad (2)$$

Equations (1) and (2) converge only very slowly for short times, and the corresponding solutions useful for short times are

$$\frac{M(t)}{M_\infty} = 2\sqrt{\frac{Dt}{L^2}}\left(\frac{1}{\sqrt{\pi}} + 2\sum_{n=1}^{\infty}(-1)^n \text{ierfc}\left[\frac{nL}{\sqrt{Dt}}\right]\right), \quad (3)$$

where *ierfc* is the integrated complimentary error function *erfc*, and

$$\frac{C}{C_0} = \sum_{n=0}^{\infty}(-1)^n erfc\left[\frac{(2n+1)L - x}{2\sqrt{Dt}}\right] + \sum_{n=0}^{\infty}(-1)^n erfc\left[\frac{(2n+1)L + x}{2\sqrt{Dt}}\right] \quad (4)$$

The above equations assume instantaneous achievement of the surface concentration C_0 of the penetrant, a constant diffusion coefficient, and constant volume of the polymer film. As can be seen from the small volume uptakes of Fig. 1, the later condition is certainly fulfilled.

For the tetrapolymer D of Scheme 1, the water uptake curves show an initial rapid rise, followed by a slowing of the uptake rate which results in the curve not yet approaching saturation after 300 seconds (Fig 1). Obviously this behavior is substantially more complex than a single simple Fickian diffusion process. The overall water uptake is fairly small, resulting in a thickness increase of only about 0.4% after 5 min for an initial film thickness of about 200 nm.

Attempts to fit the water uptake curve to Eq. (1) quickly show that there are three separate regions corresponding to three different diffusion processes.

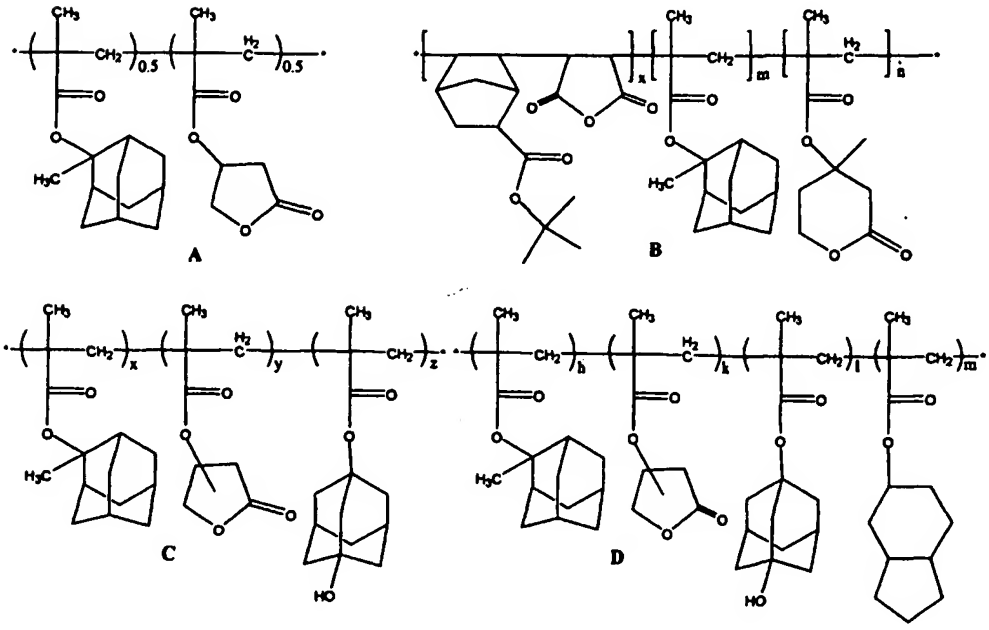

Scheme I:
Polymers A-D used in early 193 nm immersion work under the auspices of the SEMATECH 193 nm task force.

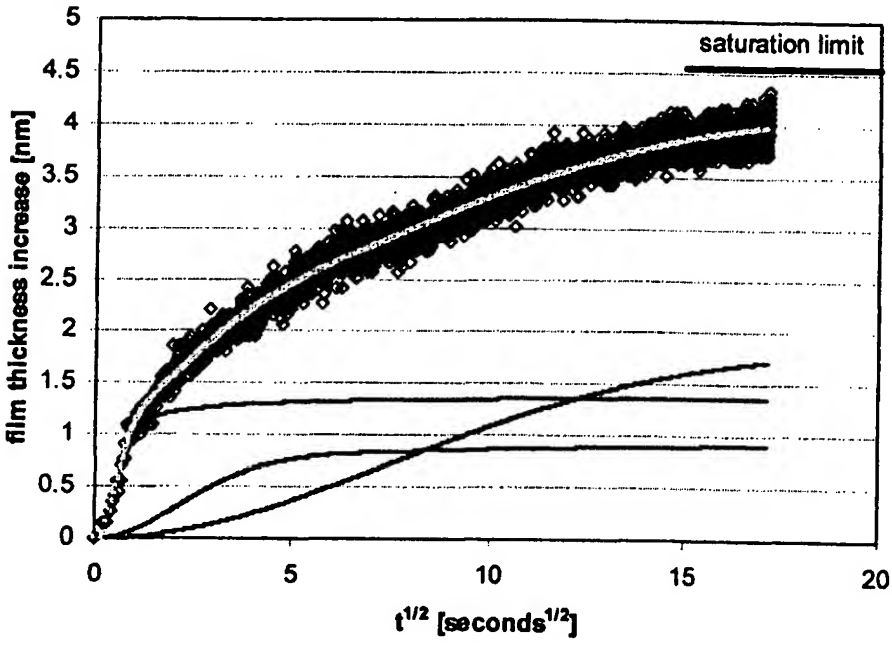

Figure 1: Water uptake of experimental resist formulation D of Scheme 1 and its de-convolution into three different processes. Initial film thickness about 200 nm.

A similar approach, combining two equations of type (1) with two different diffusion constants, has been used to describe the bimodal distribution of water in muscle tissue.[5] The total water uptake is then described by the equation

$$m(t) = \sum_{i=1}^{3} M_i(t) = \sum_{i=1}^{3} M_{\infty,i}\left(1 - \frac{8}{\pi}\sum_{m=0}^{\infty}\frac{1}{(2m+1)^2}\exp\left[-D_i\cdot(2m+1)^2\pi^2\frac{t}{L^2}\right]\right) \quad (5)$$

Table 1: Fit parameters for mass uptake from Eq. (5).

I =	$M_{\infty,i}$ [nm]	D_i [μm^2/sec]
1	1.382	0.00824
2	0.970	$4.429\cdot10^{-4}$
3	2.198	$3.634\cdot10^{-5}$

where the constants $M_{\infty,i}$ and D_i are given in Table 1. From Table 1, it is seen that even the highest diffusion constant is about 15 times smaller than the ones typically observed for water absorption from the gas phase for resists based on phenolic polymers[6] (0.1 to 0.13 μm^2/sec; see, however, work on novolak films[3] without sensitizers and other additives which found values about 3-4 times smaller). From the emerging evidence for confinement effects in thin films,[1] one

would expect that at the film thickness of 200 nm used in this study, the diffusion constants will still correspond to those found in the bulk material.

Fig. 2 shows the fit of the curve for early uptake times (t < 0.5 sec).There appears to be a small time offset about 0.03 seconds before the onset of the first diffusion process, which was taken into account for the fit.

Together, the three processes give two clearly separated regimes (Fig. 3): in the first regime (0-3 sec), where the fast process saturates, about one third of the water is taken up. The water concentration in the film is characterized by a high concentration immediately at the surface and an essentially flat profile in the bulk. In the second regime (>3 sec), the remaining water is taken up very slowly, and there is a substantial water concentration gradient deeper in the film.

Further work is needed to gain better understanding of the nature of the three observed processes on a molecular scale. It should be pointed out that the fractions of the total mass increase corresponding to the fast processes are roughly equal to the molar fractions of the hydroxyl-group and lactone-containing monomers (~30 and 20%, respectively).

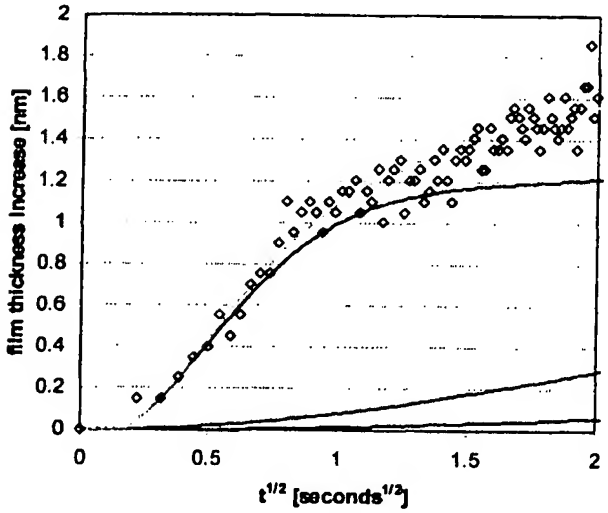

Figure 2: Water uptake at short immersion times: deconvolution into three subprocesses. Fourth curve shown is fit according to Eq. (5).

The third process may conceivably be related to diffusion through a network of less favored sites or to rearrangements in the polymer secondary structure.

The effect of refractive index changes on the aerial image resulting from water uptake into the photoresist have not yet been modeled exactly; however, it is possible to estimate the approximate size of the optical path length difference in the photoresist from the average refractive indices of the dry photoresist and the immersed resist at saturation. For the film of Fig. 2, the refractive index changes by about 0.3%, corresponding to an optical path length increase of 0.7 nm. Even if the saturation concentration of water were 10 times higher (as it is for polyhydroxystyrene), the optical path length change is still less than 6 nm. It is thus not to be anticipated that the time dependence of the resist's water uptake during immersion will lead to significant optical effects.

3. Effect of Water Uptake on Photoresist Chemistry

It has long been known in photolithography that water concentration can have significant impact on the photospeed of chemically amplified systems. In acetal type systems, water is a reaction partner in the deprotection reaction, e.g., causing hydrolysis of vinyl ether protective groups to alcohols and aldehydes. However, water plays an important role even in systems where it is not a direct reaction partner, such as

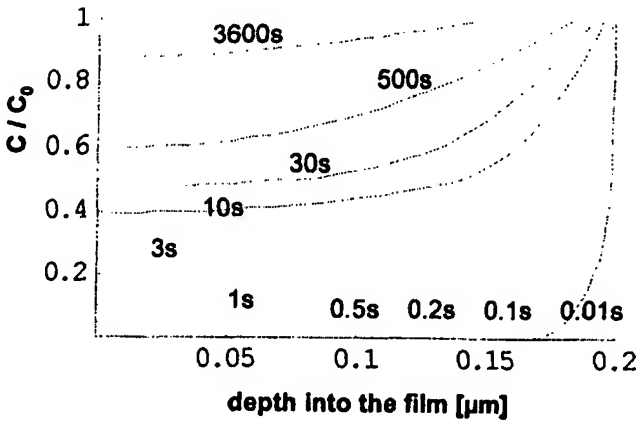

Figure 3: Water concentration profiles, relative to surface concentration, obtained from the summation of the three diffusion processes according to Eqs. (2) and (4). Wafer surface is at depth = 0 .

248 nm ESCAP systems or 193 nm photoresists, both of which rely on the acid-catalyzed cleavage of tertiary esters. In this case, water acts by reducing the acidity of the photogenerated acid by reacting with it to form a hydronium ion H_3O^+. The hydronium ion is a weaker acid than the various phenol-hydrogen ion or carboxylate hydrogen ions; in 193 nm systems where acid

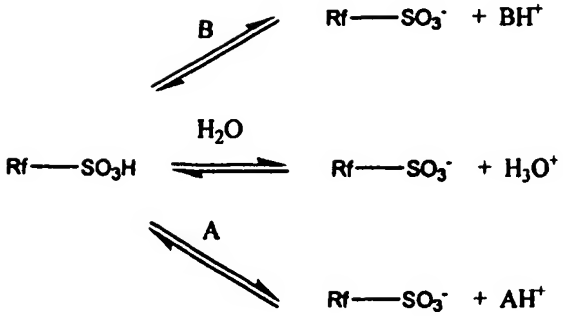

Scheme II: Effect of water on acid dissociation equilibria in resist films[7].

dissociation is not complete, it also reduces the concentration of the available undissociated acid. It has been observed that exposure in very dry nitrogen actually leads to measurable photospeed decreases of ESCAP type resist, relative to exposure at standard cleanroom humidity (as opposed to its effect in acetals, where higher humidity leads to higher photospeed). In a way the effect of water in high-activation energy systems is analogous to that of adventitious or intentionally added base quenchers, except that both its K_a value and its concentration are several orders of magnitude higher. In the case of hydroxyl-containing 193 nm polymers, e.g., the MAdMA/HAdMA/ GBLMA copolymer type of Scheme 1, the hydroxyl concentration is typically between 1 and 1.8 mmole/g polymer; a water concentration of 2% at equilibrium corresponds to about 1.3 mmole/g polymer, whereas base quenchers are measured in micromoles/g polymer (cf. Scheme II). In phenolic systems, where the relative concentrations of water and the more acidic phenols are inverted, water is seen to have a small effect. While it is thus conceivable that water may have an influence on the activity of the photoacid, it is unlikely to be a dominant effect. However, final clarification of its impact is still awaiting systematic and conclusive study.

4. Leaching of Photoresist Components into the Immersion Medium

The study of the leaching of photoresist components into the immersion medium has been one of the top priorities of the SEMATECH-led task force for immersion lithography that began its work in the fourth quarter of 2002. The three main areas of concern were optical changes in the immersion medium (mainly its refractive index), contamination of the lens by deposition of leached resist components or their photoproducts, and changes in the imaging performance of the photoresist. Of these three concerns, the first has conclusively been laid to rest: at the contamination levels seen, the refractive index change is at worst of the order of 10 parts per million, about one order of magnitude less than the changes due to the thermal effects. The second area, lens contamination, is as of this writing (Spring 2004) to a large extent still terra incognita, and the final evaluation of which level of leaching is acceptable will have to await the outcome of lens contamination studies presently under way. However, it appears probable that in the worst case, i.e., the finding that indeed unacceptable and irreversible lens contamination can occur, the outcome of the studies will be only that top barrier layers will become mandatory for 193 nm immersion lithography. While top barrier coats may add slightly to the process cost and complexity, it will be shown below that suitable materials exist, so that mandatory use of a top barrier coat cannot be considered to be at the level of a showstopper.

Of the last remaining area, the imaging impact of the leaching of photoresist components into the immersion medium, is the subject of Section 5. The remainder of this section will focus on the description of the present state of knowledge of the leaching phenomenon.

The study of leached photoresist components is faced with two general problems: finding suitable analysis methods with sufficient sensitivity and accuracy, and obtaining sufficient sample size for testing. The latter appears to be trivial; however, it is not, because due to the meniscus forces on the hydrophobic substrate, simply puddling water on coated wafer will result in a layer thickness that is a large multiple of the approximately 1 mm immersion medium thickness that is expected to be

used in production tools once they are available. Different groups have developed different solutions for this problem; Fig.4 shows our approach. Our target was to obtain as large a sample volume as possible at a realistic concentration. To this purpose, we designed and built a full-wafer immersion chamber for 8" wafers in which a

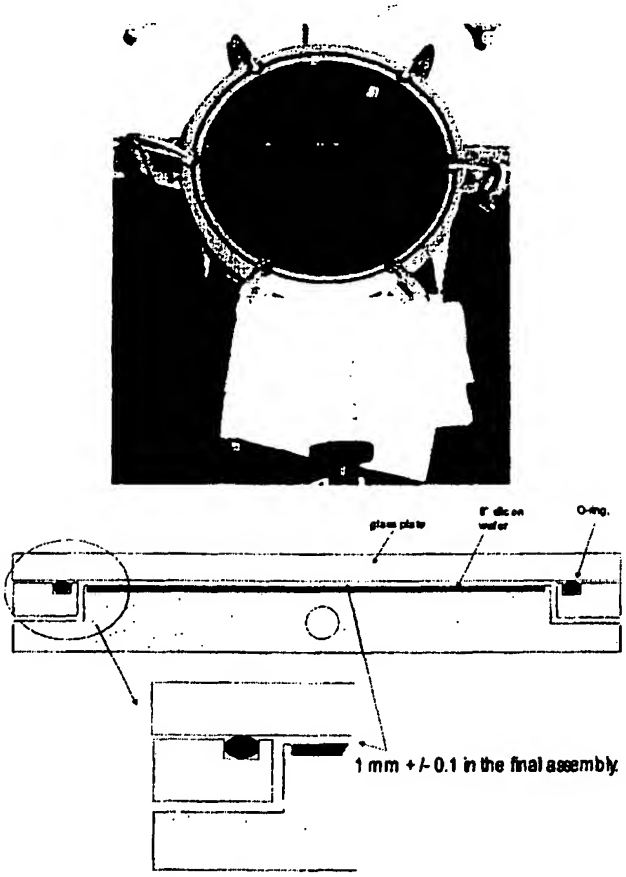

Figure 4: Full wafer immersion chamber for leaching studies. a) Photograph of partially filled wafer holder, b) cross sectional drawing. The water is injected by a syringe, with a full fill requiring about 3 sec. The water can be either pushed out through the top exit hole or be retrieved by pulling it out with the same syringe (3 sec duration) The exact water layer thickness can be calculated by the amount of water required for a full fill (ca. 35-45 ml, depending on machining tolerances). The glass plate can be replaced with a quartz plate for short wavelength flood exposures.

glass plate limits the thickness of the water layer to approximately 1 mm (Fig. 4).

Early studies using (in some cases very) small sample volumes had shown the level of contamination that could be expected to be found in the immersion medium. Work at IBM Almaden[8] ad found consistent levels of perfluorobutanesulfonate (nonaflate) anion between 70 and 130 ppb for unexposed resist, and 66 to 270 ppb for exposed resist (Table 2). However, the numbers found for amines were inconsistent. An important finding of this early study was that within the time studied, only a small fraction of the nonaflate was leached from the resist. Since only the anion was detected, it is not possible to make statements on the leaching of cation components in the exposed area (in the uneposed, it is assumed that cation and anion must leach at equal levels to maintain electroneutrality).

Table 2: Leaching levels (in ppb) found in first small volume leaching experiments as analyzed by LC/MS/MS (from ref. 8). Theoretical maximum for nonaflate: 1,800 ppb. ND: not detected.

		Nonaflate		Amine	
Resist	Time [min]	Unex-posed	Ex-posed	Unex-posed	Ex-posed
1	1	100	66	310*	ND
	15	70	88	220	ND
	90	130	270	50	ND
2	1	70	104	510	ND
	15	70	165	90**	ND
	90	130	225	ND	170

*: *exceeds theoretical maximum*

**: *below limit of quantitation (LOQ)*

Work in C.G. Willson's group at the University of Texas at Austin employed the use of radiolabeled model compounds to gauge the extent of leaching.[9]. They used triphenylsulfonium nonaflate (TPS Nf) bearing a ^{14}C label on one of the cation's phenyl rings and analyzed the level of leached radioactivity by scintillation counting. This study nicely complements the IBM Almaden work and other studies based on the detection of the PAG anion, since the combination of the two methods makes it possible to distinguish between PAG cation/anion leached in the ionic form, leached cation photodissociation products (in exhaustively exposed films), and leaching of free photoacid.

The Austin results showed a constant radioactivity in the water layer, at a level corresponding to a leached PAG weight of about 8 µg per 2" wafer, or 2.5 µg/sq.in. This result would correspond to about 125 ppb in a 1 mm supernatant water layer, which is quite consistent with the IBM results for unexposed resist. The study gave,

however, two unexpected results: first, that the level was independent of leaching time between about 30 sec (the fastest the leaching experiment could be performed) and 30 min., and second, that the level of leached activity was also independent of whether the wafers were exposed or not.

The conclusion from the first result was that PAG leaching is a fast process that saturates in less than 30 sec at a level that is a fraction of the PAG level contained in the film, leading to the conclusion that PAG cation leaching must be a surface phenomenon. In contrast, the higher levels of nonaflate leached from exposed areas mean that anion leaching reaches deeper into the photoresist and may possibly be related to photoacid mobility and diffusion. Lastly, the fact that unexposed and exhaustively exposed areas show the same level of leached radioactivity indicates that the leaching rate of the PAG cation and its photoproducts is the same.

Inspection of Fig. 5 shows that after 6 sec, about 20 ppb of nonaflate anion had been extracted, whereas after 60 sec, in the presumed region of saturation, over 250 ppb had been extracted. This indicates that this method has the potential to enable future studies of the kinetics of unexposed PAG leaching; such studies are under way.

In the exposed area, the nonaflate extraction is substantially faster: the 6 sec result is within 15% of the saturation value. This time dependence indicates that in exhaustively exposed films, anion leaching occurs on a different time scale than cation photoproduct leaching; the higher level of anion leaching again indicates that PAG diffusion and mobility play an important role.

Fig. 5 additionally shows the essentially complete suppression of leaching, both in the exposed and the unexposed area, by the use of a top barrier layer (AZ® TARP™, see Section 5). This result may be interpreted as proof-of-concept for the top barrier layer approach.

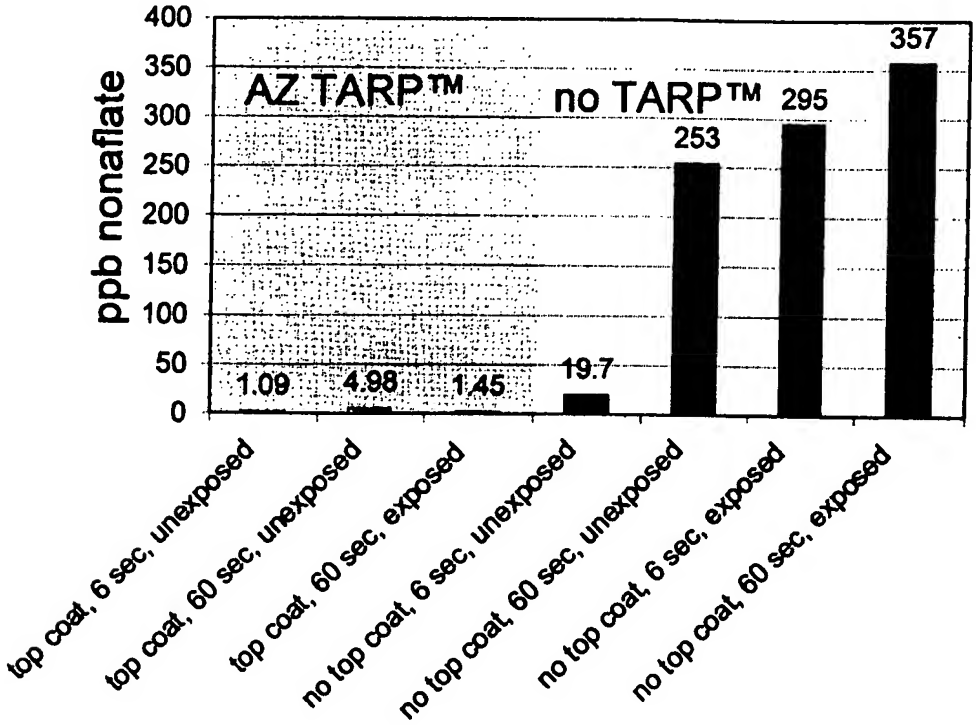

Figure 5:
Nonaflate leaching from a resist containing polymer A and 5% TPS Nf, using the immersion camber of Fig. 4. Exposed results after 248 nm flood exposure of wafers prior to immersion (ca. 200 mJ/cm^2). Top coat is AZ®TARP™, a developer-removable top barrier layer coated at 35 nm thickness. AZ®TARP™ results indicate that suppression of leaching is essentially complete; the low levels of nonaflate found are probably due to coating imperfections.

The wafer immersion chamber shown in Fig. 4 is capable of leaching experiments with up to ten times higher time resolution than previous experiments. Additionally, sample volumes are much larger, leading to better reproducibility and analytical accuracy as well as to reduced contamination sensitivity. Fig. 5 shows leaching results obtained with a photoresist containing polymer A and 5% TPS nonaflate PAG, cast from PGMEA.

The two photoresist components remaining to be discussed are base additives and solvents. There is good news from the solvent front: no trace of radioactively labeled solvents could be detected in the immersion water, which due to the high detection limit of the method

indicates that their level must be very low indeed.[10]. The situation is more murky in the case of bases, to some extent due to the lack of highly accurate and sensitive methods as well as to the sensitivity of small samples to contamination. Efforts to use radioactively labeled bases[8,9] have so far been mired in synthetic difficulties. Analytical determination of the extent of base leaching remains a task for the future; however, the lithographic evidence points towards the fact that base leaching is highly dependent on the nature of the base and can vary from very low to quite extensive.

5. Imaging of Photoresists under Immersion Conditions

5.1 Immersion Resists for Use without Top Coats

As is typical for the early stage of a new technology, 193 nm immersion has been plagued by a dearth of exposure tools. To a large extent most of the early learning has been done by simulated immersion using "dry" 193 nm tools, or on interference lithography setups, in some cases at 193 nm, in others at the slightly offset wavelength of 213 nm.[11] More recently, a first 193 nm full field scanner has become operational;[12] it is expected that over a dozen full field tools will follow within 2004 and will be used for early learning at research institutes and semiconductor manufacturers worldwide. These early tools will not yet take advantage of the resolution enhancement capabilities of 193 nm immersion, such tools (with NAs greater than 1) are only expected in mid-2005. However, they will show an enhancement of DOF by as much as a factor of two.

The origin of this DOF enhancement is the breakdown of the paraxial approximation used, for example, in the Rayleigh criteria. This breakdown means that the Rayleigh criterion for DOF

$$DOF = k_2 \frac{\lambda}{NA^2} \qquad (6)$$

needs to be replaced with a more complex formula. A number of such equations have been proposed; Eq. (7) shown below is one published by Lin.[13] The equation introduces a new factor k_3 that in the case of low NA tends towards a value of $k_2/4$:

$$DOF = \frac{k_3}{n} \frac{\lambda_0}{\sin^2\left[\frac{1}{2}\arcsin\left(\frac{1}{n}\sin\theta_0\right)\right]} \qquad (7)$$

This DOF improvement has led to strong interest in the use of early full field immersion tools with NAs smaller than unity. These tools will not show any resolution improvement but will increase DOF and hence process windows by almost a factor of 2.

Early immersion work using existing 193 nm photoresists showed that while resist performance under immersion conditions was somewhat inferior to dry results, the existing 193 nm platforms, especially the methacrylate platform, basically worked. Results were poorer for pure cycloolefin-maleic anhydride (COMA) and mixed for the hybrid COMA-methacrylate types such as polymer B of Scheme I. Quartz crystal microbalance (QCM) studies of these platforms[14] corroborated that there are differences in behavior: acrylate type resists show a small decrease in film thickness upon immersion, whereas the maleic anhydride containing types show an initial increase, corresponding to a swelling layer, followed by a larger film thickness decrease.

Examples of typical methacrylate resist performance are shown in Fig.6. A typical difference between dry and wet exposures of resists optimized for dry lithography is the tendency towards rounding of the resist tops. Fig. 6 shows a number of examples of such behavior for exposures at 213 nm (the 213 nm laser source is convenient because it naturally has a high coherence length, giving a large exposure filed, and because 193 nm resists have essentially the same absorbance at 213 nm than at 193 nm). Rounding of the resist tops implies an excess of photoacid in the upper layers of the resist, which at first glance contradicts the leaching results discussed in Section 4. However, it should be kept in mind that base leaching occurs concurrently with PAG leaching. From the lithographic results, it would appear that base leaching is quite pervasive and dominates the resist performance for resists optimized for dry lithography, where no particular attention has been paid to the water solubility of the base quenchers. Re-formulation of resists with less water soluble quenchers leads to resists that again have square tops (cf. Fig. 6 c). Studies using simulated immersion of the resist show that there is considerable leverage in modulating base solubility, but that PAG and base leaching rates need to be matched for good

lithographic performance (Fig. 7). Of course, from the point of view of contamination prevention, this means that it is preferable to have both at a low level.

Optimization of resist formulations has led to formulations that have shown good performance in interference lithography (Fig. 8), showing resolution capability of 45 nm dense lines on an immersion lithography setup at Nikon Inc. with n sin θ = 1.07. The same resist imaged on the ASML /1150i at 0.75 NA (Fig. 9) shows a potential pitfall of optimizing reists using immersion lithography: the same formulation shows considerable LER when exposed on a scanner. Presumably the difference in LER is due to the difference in aerial image quality, and LER is not visible in the immersion experiment due to the very high contrast of the interferometric image.

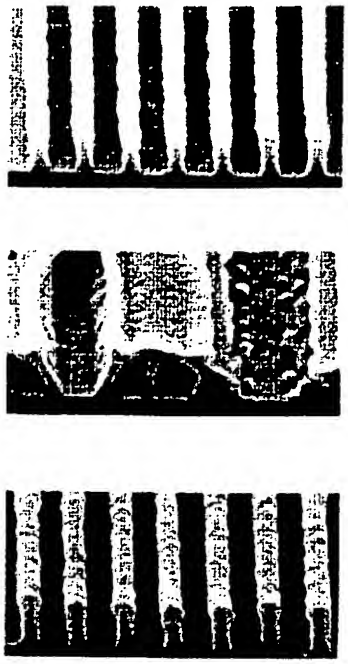

Figure 7: Example of 193 nm immersion resist formulations with mis-matched PAG and base leaching rates. Simulated immersion performed by water soak prior to development. Nikon S306C (NA= 0.78), 200 nm resist thickness on AZ® 1C5D BARC. Top: dry refe-rence, center: water soak prior to exposure, bottom: water soak with AZ® TARP™ coating.

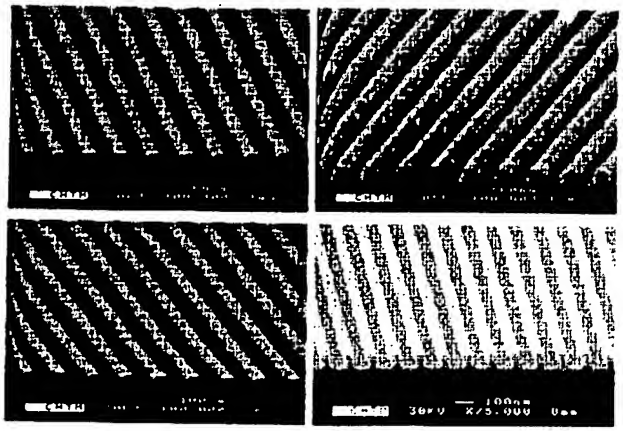

Figure 6: Examples of photoresist exposures under immersion conditions at the Univ. of New Mexico (213 nm interferometric exposure, 131 nm pitch). Top left (a): exp. resist, dry exposure; top right (b): same resist, water immersion exposure, bottom left (c): resist re-formulated to give straight tops. Bottom right (d): early exposure of AZ® AX™1040P (150 nm pitch), showing that some commercial resists can perform well without optimization.

Figure 8: Performance of optimized formulation in interference lithography. Immersion exposure at Nikon, Inc. with n sin θ = 1.07, without top barrier layer. Exposure on BARC, resist thickness 100 nm.

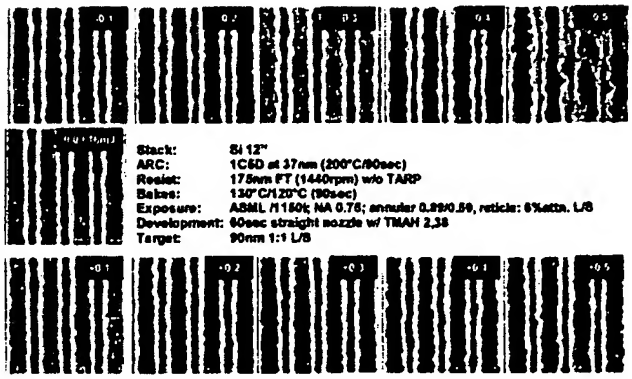

Figure 9: Immersion exposure on ASML /1150i (0.75 NA)of the same formulation as in Figure 9. 90 nm structures in 175 nm resist, attn PSM, annular illumination 0.89/0.59, 16 mJ/cm^2.

5.2 Top Barrier Coats for Immersion Lithography

One possible solution to the leaching and water diffusion issues is the use of top barrier coatings. Such coatings isolate the resist layer from the immersion medium and thus can in principle make it possible to use existing resist formulations with no or only minimal formulation optimization.

Proof of principle has been established with a first such coating[13] using a developer-insoluble fluoropolymer that has to be applied and removed with a perfluorinated solvent (a perfluoroalkylamine and perfluorobutyltetrahydrofuran, respectively). However, such a process is widely considered to be unacceptable for production implementation due to the added complexity of the top layer removal, the cost and possible environmental impact of the solvents, and the danger of introducing solvent rich hydrophobic layer at the resist top. A successful process must be modeled on more acceptable technologies, for example, that of the top antireflective coatings widely used in lithography today. These materials are non-tacky after spin on from water, i.e., they do not require a bake after spin-on, and are removed in the developer. They only add minimal process complexity (a single spin step) to the process.

A commercially successful top barrier layer should therefore also be developer soluble. However, it is challenging to design a system that can be spun on from water, then is completely water insoluble without a bake step, and can then be removed without problems in the developer. Relaxing the spin-on solvent requirement makes it possible, though, to design systems that can be spun on from organic solvents that do not attack photoresist. A process flow for such a material is shown in Fig.10; only a single spin step is added to the process.

Figure 11 shows the performance of such a material, which we have introduced under the name of AZ® Top Anti-Reflective Protective coating, or AZ® TARP™ coating. AZ® TARP™ coating is highly soluble in all investigated EBRs and does not require modification of the develop process. Moreover, it is highly transparent at 193 nm and also functions as an antireflective coating with near-perfect swing suppression. The present formulation still shows evidence for increased bridging at high defocus; work is under way to resolve this issue in future formulations.

The optimum refractive index for a top antireflective coating is the geometrical mean of the two adjacent layers:

$$n_t = \sqrt{n_m n_r} \qquad (8)$$

where the indices stand for t: top layer, m: (immersion) medium, and r resist. For dry lithography, the antireflective layer is bordered by air (n = 1) and photoresist (n = 1.7), so that the top ARC would need to have a refractive index of around 1.3 to be fully capable of suppressing the swing curve. Only highly fluorinated polymers come close to that value,

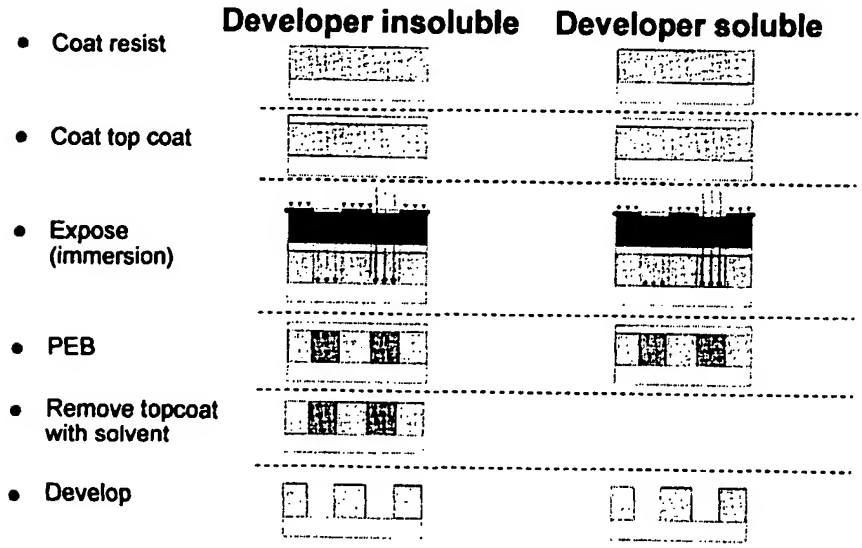

Figure 10 (left):
Process flow for developer insoluble and developer soluble top barrier layers. To achieve minimal added process complexity, it is desirable that the top layer does not require a bake after spin-on and does not have to be removed prior to the PEB; it should dissolve during the development step without process changes.

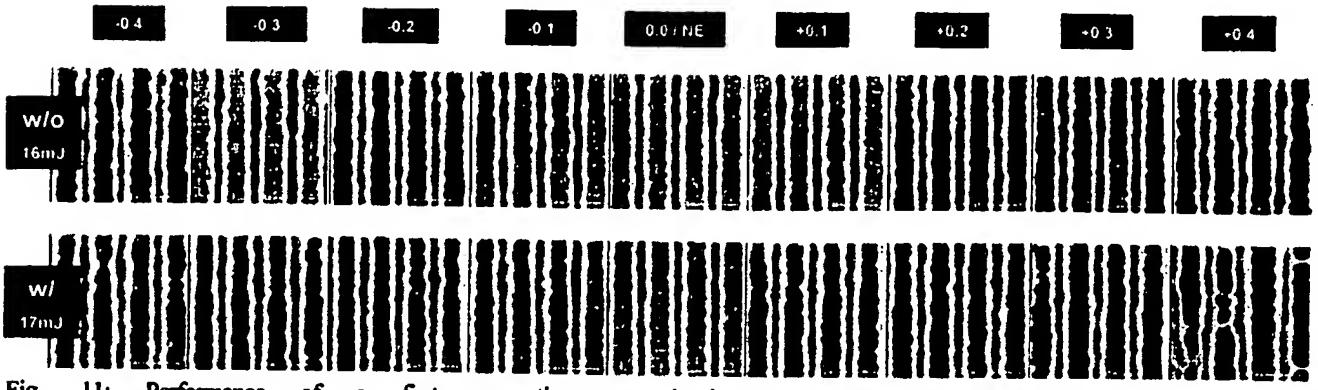

Fig. 11: Performance of a first generation top barrier layer for immersion lithography. The AZ® TARP™ 1 material shows good compatibility with the resist, although there still is some evidence for increased bridging at the edge of focus.

and they are not compatible with the water or developer processing requirement discussed earlier. For immersion lithography, however, the topmost medium is water, with a refractive index of 1.44; for this case, Eq. (8) gives an optimum value of 1.56, a value that is in a range that can be achieved by a number of developer-soluble polymers. The refractive index of AZ® TARP™ coating is close to the theoretical optimum; Fig. 12 shows a calculation of film stack reflectivity into water as a function of TARP™ thickness for an angle of incidence of 45°, corresponding to a NA of about 1.2. At this angle, the TM polarization of light contains zero image information, but is fully coupled into the resist. The reflectivity of the valuable TE polarization is lower for water immersion than it is into air, even without TARP™ coating (thickness = 0), a result of the improved match between refractive indices in the case of immersion. Still, maximally 2.5% of the incoming TE light can be reflected off the film stack into water. Use of an optimized top antireflective coating would couple this light into the film as well. If randomly polarized light is used, a reduction of the TE reflectivity not only leads to a swing improvement, but also improves image contrast by maximally 2.5%/2 = 1.25%, unlike in the case of AR coatings for low NA lithography, where the aerial image quality is unaffected by the top coat.

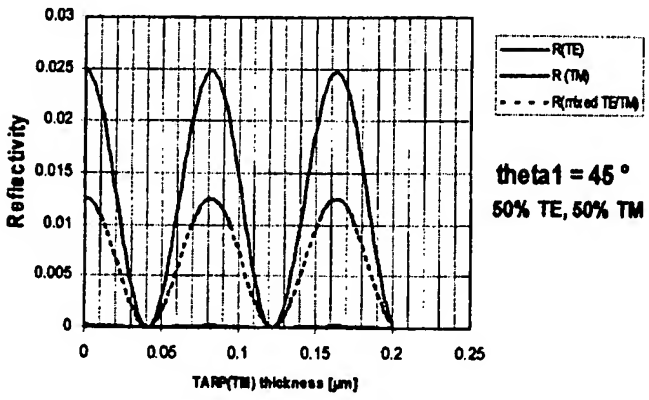

Figure 12: Suppression of TE light reflection by AZ® TARP™ 1 material (see text)

The future of top barrier layers is currently unclear. It is the industry's stated general preference not to use top barrier layers in production unless their use cannot be avoided. However, there currently is still insufficient information to tell whether this will be possible. The work done so far gives rise to a high level of confidence that such layers will be available if they are required.

5.3 Bottom ARCs for Immersion Lithography

With immersion lithography, the range of angles that incoming rays form with the resist or BARC surface is greatly increased. For an NA of 1.2, the maximum angle, achieved for features at the resolution limit, is 45°; at the same time, large features will result in much smaller diffraction angles, and the light will fall onto the imaging plane at almost vertical incidence. A result of this is that the optical path length of the rays from small features in resist and BARC will be 41% longer than that of large features.

A result of this is that BARC thickness becomes a function of diffraction angle and hence feature size. Figs. 13 and 14 show this dependence on the angle. In interference lithography, where only a singe pitch is imaged in each experiment, it is possible to adjust the BARC thickness to its correct value; however, this is generally not possible for masked exposures which usually combine are different feature sizes and pitches.

Solutions to this issue involve more complex bottom antireflection strategies, from bilayer BARCs to graded BARC layers in which the refractive index of the BARC is varied as a function of distance from the wafer surface. Both solutions have been shown by simulations to result in excellent control of reflectivity through a large range of angles; additionally, the different reflectivities of TE and TM light are controlled as well, which may be of interest if high NA scanners should not use polarized exposures.

Blayer BARCs are easiest to implement: solutions exist for inorganic on inorganic, organic on inorganic, and organic on organic BARCs. Typically, the absorptivity of the lower BARC layer is chosen to be high, and the upper BARC layer has a lower reflectively. One such

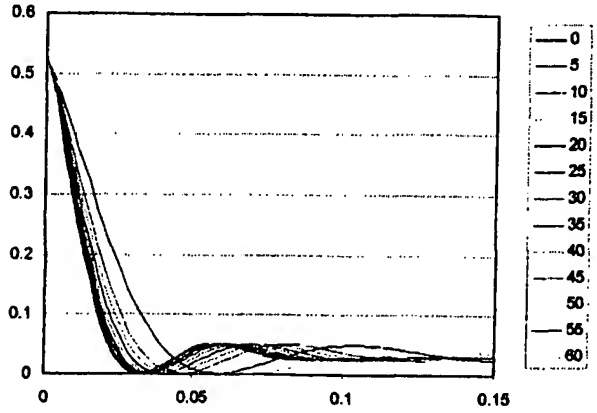

Figure 13: Angle dependence of BARC reflectivity into the resist for vertical (=0) and non-vertical (>0) incidence.

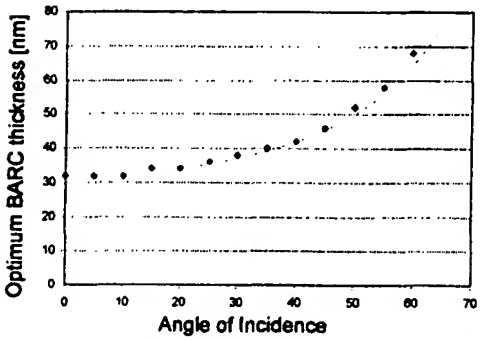

Figure 14: Position of minima for reflectivity curves of Fig. 13. Solid line shows initial thickness divided by cos θ.

commercial upper BARC material, AZ® 2PLK BARC, is optimized for work on SiON and shows a k value of 0.2.

6. Challenges for the Extension of 193 nm Lithography

6.1 Collapse Behavior of 193 nm Resists at Small Feature Sizes

A common observation of resist behavior at the small feature sizes achievable with immersion technology is a strong tendency towards collapse even at aspect ratios below 3 which have historically been considered "safe." It is of course well known that the Laplace pressure leading to the collapse of small features is inversely proportional to the line spacing:

$$\Delta P = \frac{2\gamma \cos\theta_w}{d} \qquad (9)$$

where γ is the surface tension, θ_w is the contact angle of water on the resist, and d stands for the space width. Eq. 9 indicates that the collapsing force increases by 80% going from 100 to 55 nm lines; however, 157 nm resists have historically not shown this kind of issue at the same feature size (Fig. 15). The explanation for the different behavior of 193 and 157 nm resists lies in the different hydrophobicity of the platforms: the contact angle of the 193 nm resist is substantially lower than that of 157 nm resists (Table 3), making the force 2x higher. A more hydrophobic 193 nm resist would reduce collapse issues; however, it is not clear that pursuing such an approach would not lead to a negative impact on lithographic performance.

Figure 15: Comparison of collapse behavior of 157 and 193 nm photoresists. 55nm features, non-immersion. Left: 157 nm exposure on Exitech ministepper at SELETE, NA=0.9, alt.PSM; right: 213 nm interference lithography at U. New Mexico.

Table 3: Typial contact angles of photoresists

193 nm unexp.	193 nm exp.	157 nm
52	48	73

6.2 Extension of 193 nm Immersion Lithography: "Flavored Water"

The use of immersion fluids with refractive indices higher than water has been discussed as a possible avenue to extend 193 nm immersion technology to even smaller features. In an exposure system with a non-planar last lens element, the maximum possible NA is given by the minimum of the refractive index of the immersion medium and of the photoresist. Since the photoresist refractive index at 193 nm is roughly 1.7, it is possible to build exposure tools with NAs up to 1.7 if a suitable immersion medium is found. Since water has many properties that are highly desirable in an immersion medium, this work has mostly focused on aqueous solutions ("flavored water").

Many of the solutions currently studied for proof of principle contain known contaminants such as alkali metals, have high absorbance, or both. Examples include cesium sulfate and organic dyes that work by raising the refractive index by anomalous dispersion. The most practical solution described so far may very well be 17% phosphoric acid, which combines low absorbance with a high refractive index of 1.65. Scanners with such a high numerical aperture would easily extend the life of 193 m immersion lithography to the 32 nm node. However, it will be practically challenging to build scanners to work with corrosive immersion medium and to make photoresists work with a highly acidic immersion medium; on top of everything, phosphorous is also a semiconductor dopant.

It should also be noted that even if a suitable high-refractive index medium is found, building such hyper-NA tools is by no means a done deal. Besides the massive size of such lenses, it has to be noted that non-planar last lens elements may bring with them substantial hydrodynamic complications during the scanning motion. If the last lens element needs to be planar, the maximum possible NA is the minimum of the refractive index of the last lens element, the immersion medium, and the photoresist. Unless a lens material with a substantially higher refractive index than fused silica is developed (e.g., sapphire), the possible increase in the possible maximum NA is going to be quite limited.

There is, however, a benefit associated with high refractive index liquids that is not limited by the above considerations. DOF improves with the use of high r.i. liquids, and this improvement is not limited by the limitations placed on NA by the refractive index. Fig. 16 shows the result of simulations of the dependence of DOF on the index of the immersion medium at a fixed NA of 1.2. As can be seen, DOF continues to increase even if the refractive index of the medium exceeds that of the lens or of the photoresist.

Overall the benefits of high refractive index immersion media are sufficiently large to provide a strong incentive for their implementation, making it highly probable that an acceptable technical solution will be developed. Certainly the alternative technologies, Extreme UV and 157 nm immersion, face at least as large technical challenges of their own.

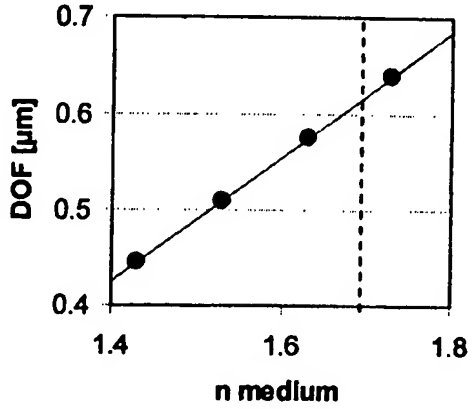

Figure 16: DOF improvement by high refractive index immersion liquids. Note that the improvement is not limited by the resist refractive index of 1.7.

6.3 Other Challenges for 193 nm Immersion Extension

As 193 nm immersion prepares to move along the roadmap, it faces many challenges, some of which arise from known roadmap requirements such as LER improvements, PEB sensitivity, and defectivity. These roadmap requirements driven by device requirements and thus are to a large extent independent of the technology that is employed in the photolithography step. Meeting these ever more stringent requirements in a timely manner is going to be a major challenge for materials suppliers; much has been written about these issues already, and it need not be repeated here.

Beyond these "known unknowns," there is a class of new and unexpected phenomena that occur as we shrink the feature size; these could be called the "unknown unknowns." In a way, the line collapse phenomenon was

the first such effect found: initially essentially unknown at 248 nm, it became a major concern for the 90 nm node, and its severity can only continue to increase (cf. Section 5.3) . Fundamental concerns have been raised about the extendibility of chemically amplified resists: some resist chemists believe image blur issues that are inherent in chemical amplification may make its utilization impractical below 45 nm. Thin films have been shown to show dramatic changes in material constants such as diffusion coefficients, glass transition temperatures, or mechanical strength once film thickness drops below a certain threshold value. The thresholds for these confinement effects are not the same for all phenomena; diffusion coefficients may change at one and glass transition temperatures at another critical film thickness value. However, the threshold-like behavior due to these thin film confinement effects is a general theme, and steep changes are commonly seen at 150 to 20 nm thicknesses. As we shrink resist thickness, resist chemists must learn to live with and maybe even use these new phenomena that not only constitute a threat but also an opportunity: for example, reduction in diffusion constants of thinner films may lead to more line edge roughness, but it will at the same time reduce the impact of diffusional image blur in chemically amplified resists.

7. Conclusion

Overall, the challenges facing materials for 193 nm immersion technology do not appear to be insurmountable, although it is a safe bet to say that we will probably still face a number of unpleasant surprises along the way. It is in our favor that in the materials area, as already the case for the optics, pellicles, lasers, etc., there is a high level of 193 nm dry expertise that we can build on. With the assistance of institutions such as SEMATECH, IMEC and SELETE that provide exposure capabilities and opportunities for early learning, there is cause for optimism that the international resist community can rise to the challenge in a timely manner.

8. Acknowledgement

This keynote lecture would not have been possible without drawing on the work of many others who have been instrumental in developing our present knowledge of the issues pertinent to 193 nm immersion technology. The authors would like to acknowledge the work of a large number of collaborators and partners, beginning with International SEMATECH, in particular Will Conley, followed by, in no particular order, Alex Raub and Steve Brueck of the University of New Mexico, the IBM Almaden research team, in particular Bill Hinsberg, C.G. Willson, his group and collaborators at the University of Texas at Austin, V. Prabhu, Erin Jablonski and the team at the National Institutes of Standards (NIST), Infineon AG, in particular Michael Sebald and Christoph Hohle, Bruce Smith of the Rochester Institute of Technology, the immersion teams of Nikon and Canon, and ASML's immersion team in Veldhoven, Netherlands.

8. References

1. L. Singh, P.J. Ludovice, C.L. Henderson, Thin Solid Films 449, 231–241(2004); Proc. SPIE 5376 (2004), in print; C.L. Soles, J.F. Douglas, E.K. Lin, J.L. Lenhart, R.L. Jones, W.-Li Wu, D.L. Goldfarb and M. Angelopoulos, J. Appl. Phys. 93, 1978-1986 (2003).

2. W. Hinsberg, G. Wallraff, C. Larson, B. Davis, V. Deline, S. Raoux, D. Miller, F. Houle, H. John, L. Sundberg, R. Dammel, and W. Conley, Proc. SPIE 5376 (2004), in print.

3. C.M. Berger, C.L. Henderson, Proc. SPIE 5039, 984-995 (2003)

4. J. Crank, "The Mathematics of Diffusion", Oxford University Press, New York 1956 (paperback edition 1999, ISBN 0 19 853411 6), p. 47ff, p. 238.

5. A.C. Jason and G.R. Peters, J. Phys. D6, 512 (1973)

6. Francois Sebillote, Andre Weill, Patrick Paniez, "Cinetique de la diffusion de l'eau dans un film mince de photoresist", Makromol. Chem. 186, 1695-1699 (1985); Yuko Shibayama, Masakatsu Saito, "Influence of Water on Photochemical Reaction of Positive-Type Photoresist", Japanese Journal of Applied Physics 29 (10), 2152-2155 (1990); Lehar, Octavia P.; Spak, Mark A.; Meyer, Stephen; Dammel, Ralph R.; Brodsky, Colin J.; Willson, C. Grant. Resist rehydration during thick film processing. Proceedings of SPIE-The International Society for Optical Engineering (2001), 4345 (Pt. 1, Advances in Resist Technology and Processing XVIII), 463-474.

7. J. March, "Advanced Organic Chemistry, Reactions, Mechanisms and Structure, Third Edition, John Wiley & Son 1985, p. 220-221

8. W. Hinsberg, G. Wallraff, C. Larson, B. Davis, V. Deline, S. Raoux, D. Miller, F. Houle, H. John, L. Sundberg, Presentation at the 2nd Intl. Sematech Immersion Lithography Workshop, Almaden, July 2003; see also ref. 2.

9. J. C. Taylor, C. R. Chambers, S. D. Burns, C. G. Willson,

Proc. SPIE 5376, (2004), in print.
10. R. J. LeSuer, F. F. Fan, A. J. Bard, C.G. Willson, C. Taylor, P. Tsiartas, W. Conley, G. Feit, and R. Kunz, Proc. SPIE 5376, (2004), in print.
11. A.K. Raub, S. Brueck, A. Romano et al., Proc. SPIE 5376, (2004), in print.
12. D. G. Flagello, B. Arnold, S. Hansen, M. Dusa, J. Mulkens, P. Jenkins, ASML; R. Garreis, Proc. SPIE 5377, (2004), in print.
13. B.J. Lin, JM3 1(1), 7-12 (2002)
14. T. Hirayama, Presentation at the 2nd Intl. Sematech Immersion Lithography Workshop, Almaden, July 2003